NASA Technical Memorandum 88230

Biogeochemical Cycling in the Ocean

Part I: Introduction to the Effects of Upwelling Along the West Coast of North America

John T. Howe

May 1986

NASA
National Aeronautics and Space Administration

NASA Technical Memorandum 88230

Biogeochemical Cycling in the Ocean

Part I: Introduction to the Effects of Upwelling Along the West Coast of North America

John T. Howe, Ames Research Center, Moffett Field, California

May 1986

National Aeronautics and
Space Administration

Ames Research Center
Moffett Field, California 94035

SUMMARY

Coastal upwelling is examined as it relates to the cycling of chemical species in coastal waters along the west coast of the North American continent. The temporal and spatial features of upwelling phenomena in the Eastern boundary regions of the North Pacific Ocean are presented and discussed in terms of upwelling episodes. Climate conditions that affect upwelling include: thermal effects, wind-induced shear stress which moves surface layers of water, and the curl of the wind stress vector which is thought to affect the extent and nature of upwelling and the formation of offshore convergent downwelling fronts. These effects and the interaction of sunlight and upwelled nutrients which result in a biological bloom in surface waters is modeled analytically. The roles of biological and chemical species, including the effects of predation, are discussed in that context, and relevant remote sensing and in situ observations are presented. Climatological, oceanographic, biological, physical, chemical events, and processes that pertain to biogeochemical cycling are presented and described by a set of partial differential equations. Simple preliminary results are obtained and are compared with data. Thus a fairly general framework has been laid where the many facets of biogeochemical cycling in coastal upwelled waters can be examined in their relationship to one another, and to the whole, to whatever level of detail or approximation is warranted or desired.

SYMBOLS

a	coefficient in eq. (12), defined by eq. (19)
B	biomass concentration
$\underline{B}$	threshold biomass
b	coefficient in eq. (13)
C_D	drag coefficient
c	mass fraction of species i, proportionality coefficient for wind velocity, eq. (16)
c_p	specific heat at constant pressure
D	diffusion coefficient

d	particle size
d_e	depth of euphotic layer
f	Coriolis parameter
g	gravitational constant
I_R	intensity of radiation backscattered upward (-z direction)
I_T	intensity of radiation transmitted in +z direction in sea
i	small distance from coast where properties are known
J_i	negative rate of predation of species i per unit mass
K_ν	Kubelka-Munk absorption coefficient at frequency ν
k	eddy conductivity
$\vec{k}$	unit vector directed vertically
P_m^B	specific biomass production rate at optimal light intensity
$\vec{M}$	Ekman mass transport, eq. (10)
m	slope of linear variation of wind, eq. (16)
n	index of refraction, compatibility condition fraction
p	pressure
Q_r	defined by eq. (25)
q_r	radiative flux
R	component of frictional force per unit volume
r_m	maximum ration for zooplankton grazing
s_1	scattering coefficient at frequency ν
t	time
U	air velocity in x-direction
$\vec{u}$	mean horizontal velocity in water, eq. (35)

u water velocity component in x-direction

V air velocity in y-direction

$\vec{V}$ horizontal air velocity (fig. 8)

$\vec{V}_{adj}$ adjusted horizontal air velocity (fig. 8)

v water velocity in y-direction

v_e water velocity in eastward direction

w water velocity in z-direction

x,y orthogonal sea surface coordinate directions

z coordinate measured downward from sea surface

α initial slope of specific photosynthesis rate at irradiance near zero

ε distance offshore where weather data are known

δ distance offshore where convergent downwelling front is located

ϕ latitude

μ radiative absorption coefficient

ρ density, reflectivity

σ zooplankton grazing rate constant

$\vec{\tau}$ shear stress vector

ω_i production rate of species i, per unit volume

Ω angular velocity of rotation of Earth

Subscripts:

a air

B blackbody

H horizontal component

i species i

o	value at, or near, coast, value at ocean surface
pm	particulate material
r	radiative, or residence time
s	surface value, scattering
t	terminal (settling velocity, eq. (20))
v	vertical component
x	component in x-direction
y	component in y-direction
z	component in z-direction
ν	spectral frequency
δ	value at offshore front

INTRODUCTION

Scientists tend to see things in bits and pieces, and understandably so. Creation is so complicated and is interdependent in such subtle ways that it is a considerable task to become proficient in one narrow aspect of scientific study. This may be especially true in the marine sciences. With respect to biogeochemical cycling in Eastern boundary currents, or coastal upwelling, it is no longer sufficient to look at bits and pieces unrelated to the whole that is there. The effects of climatology, oceanography, biology, physical and chemical events, and processes should be examined together. It would be useful to develop a framework which relates all these parts to see where they fit, in order to begin to assess their relative importance (some may not be important at all), and to ask or answer questions concerning events that affect the entire ecosystem.

Although runoff of water from landmasses into the oceans is a contributing factor toward the overall chemical budget in the seas, coastal upwelling is generally considered to be the dominant mechanism for biogeochemical cycling along much of the west coast of North America. In the upwelling process, cold nutrient-rich water is drawn from the depths and is exposed to sunlight in the euphotic zone. Phytoplankton seed germinates there and grows by uptake of upwelled nutrients (derived in part from bacterial decomposition of organic matter on the shallow continental shelf), and it in turn is grazed upon by zooplankton in a complicated

interrelated process. The process is highly variable both temporally and spatially.

Nevertheless, extensive literature exists about the various facets of the problem and we can formulate our thinking in specific and useful ways. In the context of this study, many disciplines are involved: fluid dynamics; radiative transfer; transport of, and finite rate changes in, chemical specie concentrations; photo and biochemical processes; satellite and airborne sensing; and a host of others. Clearly, we must avoid trying to describe any one discipline in such detail that precludes a useful description of the overall biogeochemical system.

For present purposes, we make every reasonable simplification to arrive at a description of the gross behavior of the system, and to reveal particular gaps in our understanding where useful research can be defined that would advance our understanding of biogeochemical cycling in the sea. We begin by considering the spatial and temporal gross features of upwelling.

COASTAL UPWELLING ALONG THE WEST COAST OF NORTH AMERICA

Ocean and weather phenomena are interdependent. Figure 1 shows a modified National Oceanographic and Atmospheric Administration sea surface thermal analysis. The solid lines show temperature contours for 1984. Part a of the figure corresponds to early summer (May 8), at which time a weak thermal front (considered to be upwelled water) existed along the coast from Point Conception to Point Arena. Part b corresponds to winter (December 7). The sea surface temperature is lower, and there is no thermal front noted. We have added to that figure (obtained from ref. 1) to show isotherms from comparable times of the year 9 yr earlier (interpolated from ref. 2), as shown by the dashed lines. Generally, the ocean appears to be 1° to 2°C warmer in 1984 than it was in 1975. This may be an artifact from the warm El Nino current which first appeared in May of 1982, and was still evident in 1983 and part of 1984. That current raised the ocean temperature as much as 5°C, and globally wreaked havoc with the weather. The amount of energy represented in 1° temperature change is enormous; the equivalent of raising the body of water to an altitude of 427 m.

As indicated by figure 1a, the dominant upwelling on the west coast of North America occurs in the spring and summer of the year. Long-term climatic data show that the wind tends to have a component that is directed toward the equator during that time. The wind, combined with the Coriolis effect of the rotation of the Earth tends to move surface waters in an offshore direction. These waters are replaced by cooler water drawn from the depths, which brings the ingredients for a biological bloom into the sunlit surface layers. At any latitude, the upwelling is intermittent as the wind varies, but the general effect is one which produces a biomass that

ORIGINAL PAGE IS
OF POOR QUALITY

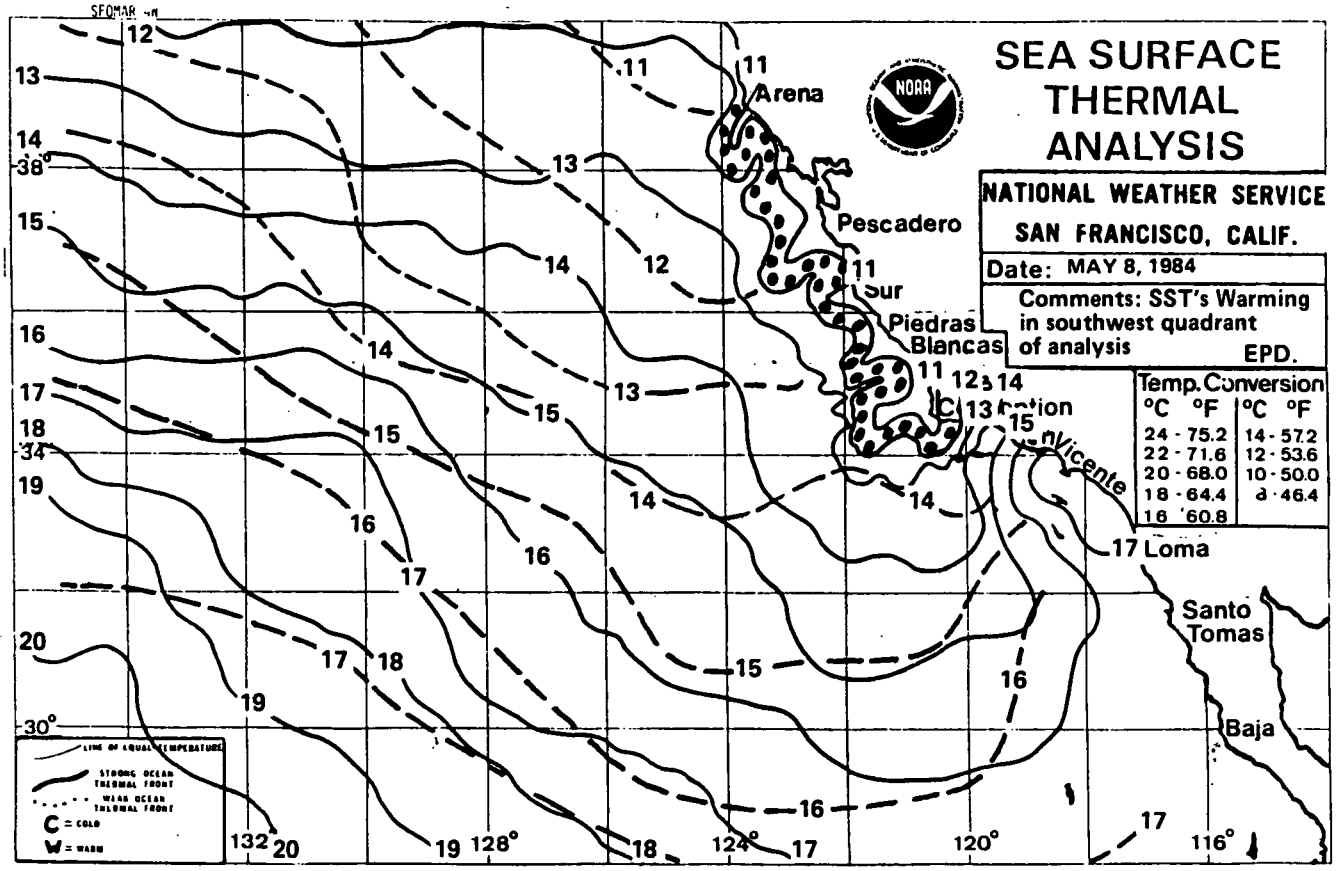

MAY 1-15, 1975 (INTERPOLATED NOAA/NMFS, REF. 2) — — —

(a) May 8, 1984 solid contours; May 1 to 15, 1975 (dashed contours interpolated, ref. 2).

Figure 1.- Sea surface thermal analysis.

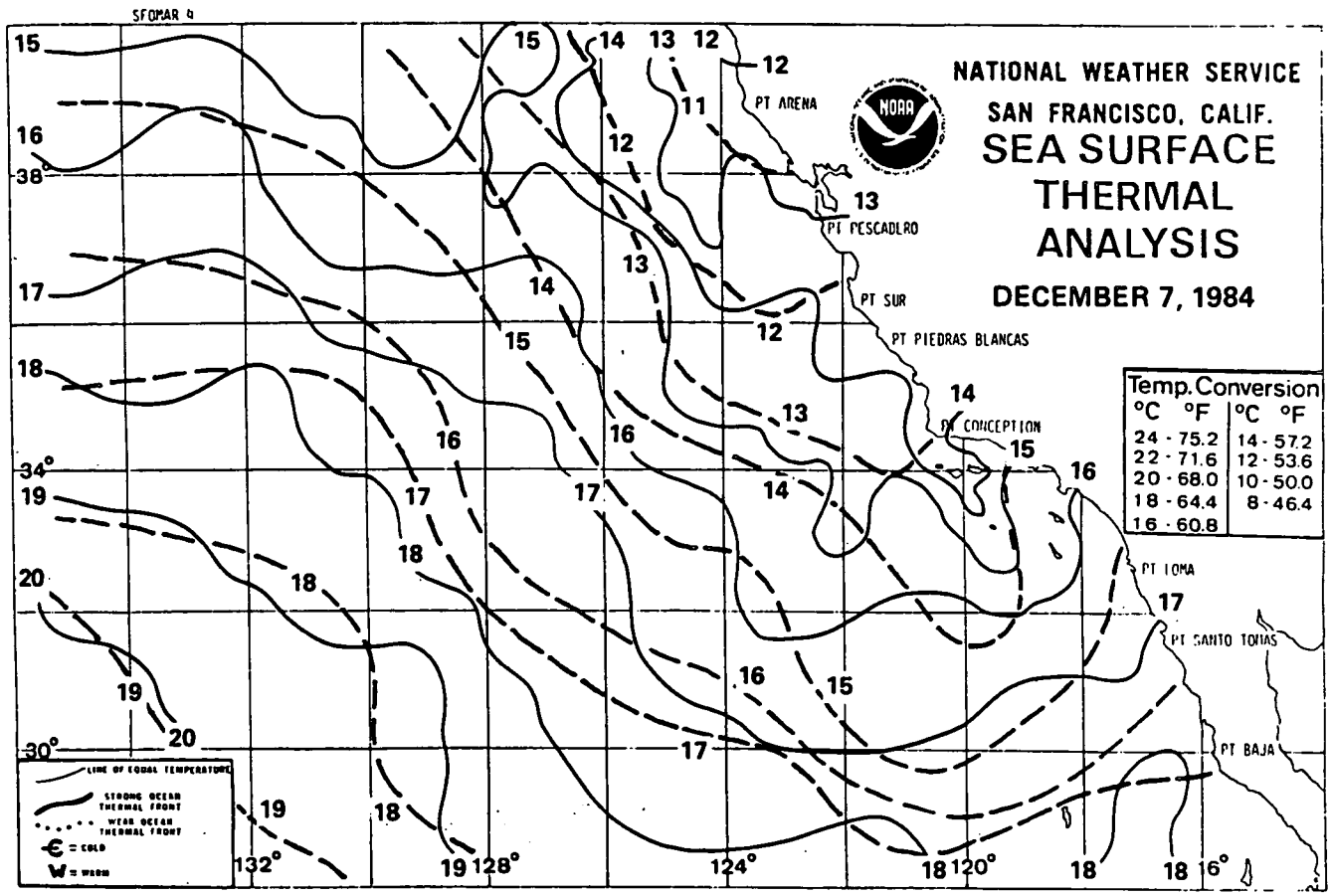

DEC 1-5, 1975 DATA (INTERPOLATED NOAA/NMFS, REF. 2) — — —

(b) Dec. 7, 1984 solid contours; Dec. 1 to 15, 1975 (dashed contours interpolated, ref. 2).

Figure 1.- Concluded.

moves sluggishly offshore. Figure 2 is a computer-enhanced infrared satellite photograph of upwelling along the coast of Northern California (ref. 3). The light tones indicate cool upwelled water, which forms irregular patterns or tongues and swirls as it moves offshore and mixes with the coastal California current.

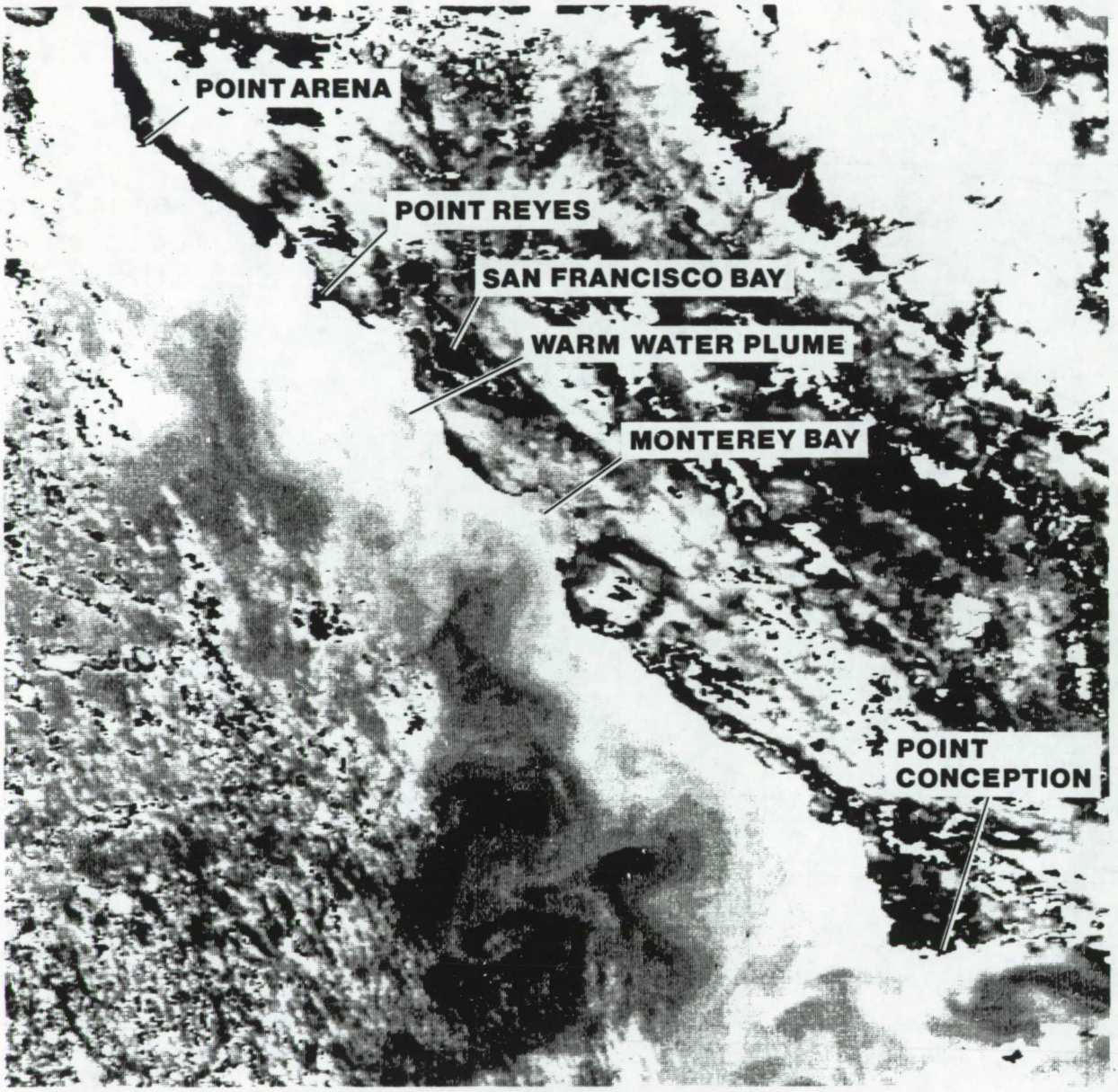

Figure 2.- Computer-enhanced infrared satellite image of California coast, May 5, 1984 (NOAA). Light tones along the coast are cool, upwelled water.

Biologically, the coastal upwelling is very important. A record marketable world fish catch of 80 million tons was made in 1984 (ref. 4). It has been estimated that half of the world's fish catch is obtained from 0.1% of the ocean area--that which is affected by coastal upwelling (ref. 5).

The intensity of upwelling varies both spatially and temporally. Figure 3 shows the 20-yr mean monthly upwelling index (defined subsequently) as a function of time for two coastal locations; the solid line corresponds to Point Sal (refs. 6, 7) which is near Point Conception; and the dashed line corresponds to near Cape Blanco in Southern Oregon (ref. 6). Both locations exhibit a peak in late spring or in early summer, and a minimum near the beginning of the calendar year. However, the long-term mean upwelling at Cape Blanco occurs only from about March to October--the ocean actually downwells at the coast during the balance of the year. By contrast, the upwelling at point Sal is more intense (the peak by a factor of 2.5) and is more persistent--the long-term mean shows dominant upwelling throughout the year. At this same location, the mean hourly upwelling index computed for April 4 to 13, 1981 (ref. 7) is shown by the solid round symbol.

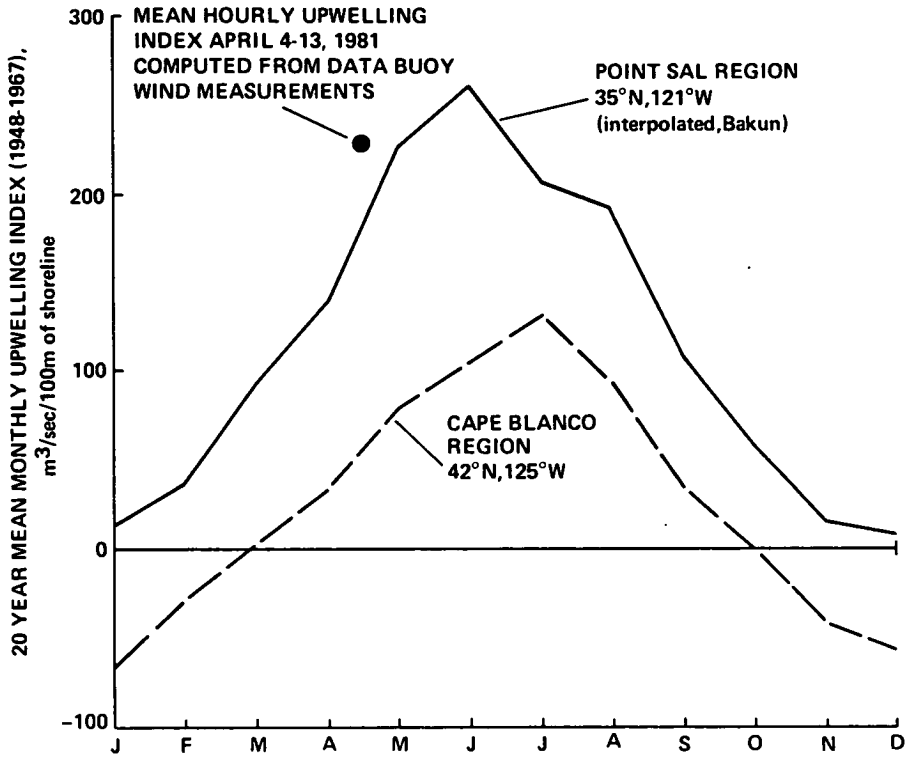

Figure 3.- Upwelling index comparison.

The detailed hourly variation of the upwelling wind (assumed to be the equator-directed component that is locally parallel to the coast (ref. 7)) is shown by the solid line in figure 4. The windspeed is highly variable, with peaks near 12 m/sec, and with the minimum near zero on April 11 (the direction was actually reversed--which was briefly conducive to downwelling). At the sea's surface, wind varies not hourly, but continuously. The variable upwelling wind causes the sea's surface temperature to rise and fall in response (dotted line, fig. 4), trending downward until the upwelling episode weakens (about April 13) as the wind level diminishes. The general decline in temperature during the episode is indicative of cooler water being drawn from the depths into the surface layers of the sea.

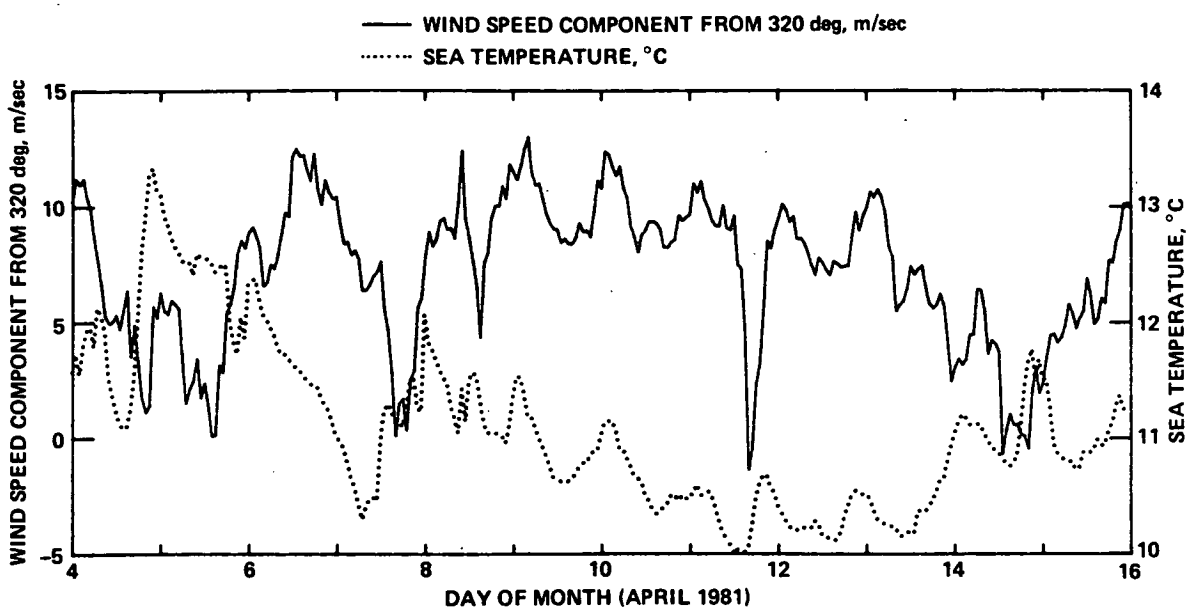

Figure 4.- Point Sal buoy data (NOAA).

The result of many such episodes is a large upwelling structure that persists far out to sea--well beyond the continental shelf, as shown by the light tones in figure 5. Some biological observations made in the "sample area" shown on the figure will be discussed subsequently.

The variation of local peak of the long-term monthly upwelling index is shown as a function of latitude along the west coast of North America by the solid line in figure 6. The peak occurs in April at the southern part of Baja California, Mexico; and progresses northward with time, as the upwelling season develops. From around Monterey Bay northward, the peak occurs in July. For the entire west coast of North America, the most intense and persistent upwelling on a long-term mean monthly basis occurs between San Diego and Point Conception. On a weekly basis (ref. 8), the maximum local peak for the year may move from 33°N to 39°N and shift from April to August in time. In 1968, 1970, and 1971 the weekly mean peaked for the year at 33°N in June, May, and June, respectively. For 1967 the yearly maximum local weekly upwelling index peaked at both 36°N and 39°N in the week of May 21. In 1969, 1972, and 1973 the weekly mean peak moved to 39°N (Point Arena--fig. 2) and occurred in August, April, and May, respectively. From the Oregon border northward, the long-term mean-upwelling index is significantly diminished, probably because of the prevailing offshore location of the atmospheric high-pressure system. Thus the Gulf of Alaska is not dominated by coastal upwelling but is dominated instead by the effects of the cyclonic gyre of the Northeast Pacific Ocean.

The dashed line in figure 6 is the latitudinal variation of the long-term mean of the curl of the wind-stress vector (ref. 9) associated with the peak upwelling index line. If the curl of the wind-stress vector is positive, the component of the upwelling wind increases offshore, and the upwelled water tends to continue to move farther offshore (fig. 7). On the other hand, if the curl is negative the upwelling

Figure 5.- Computer-enhanced infrared satellite image near Point Sal, April 13, 1981 (NOAA). Light tones along the coast are cool, upwelled water.

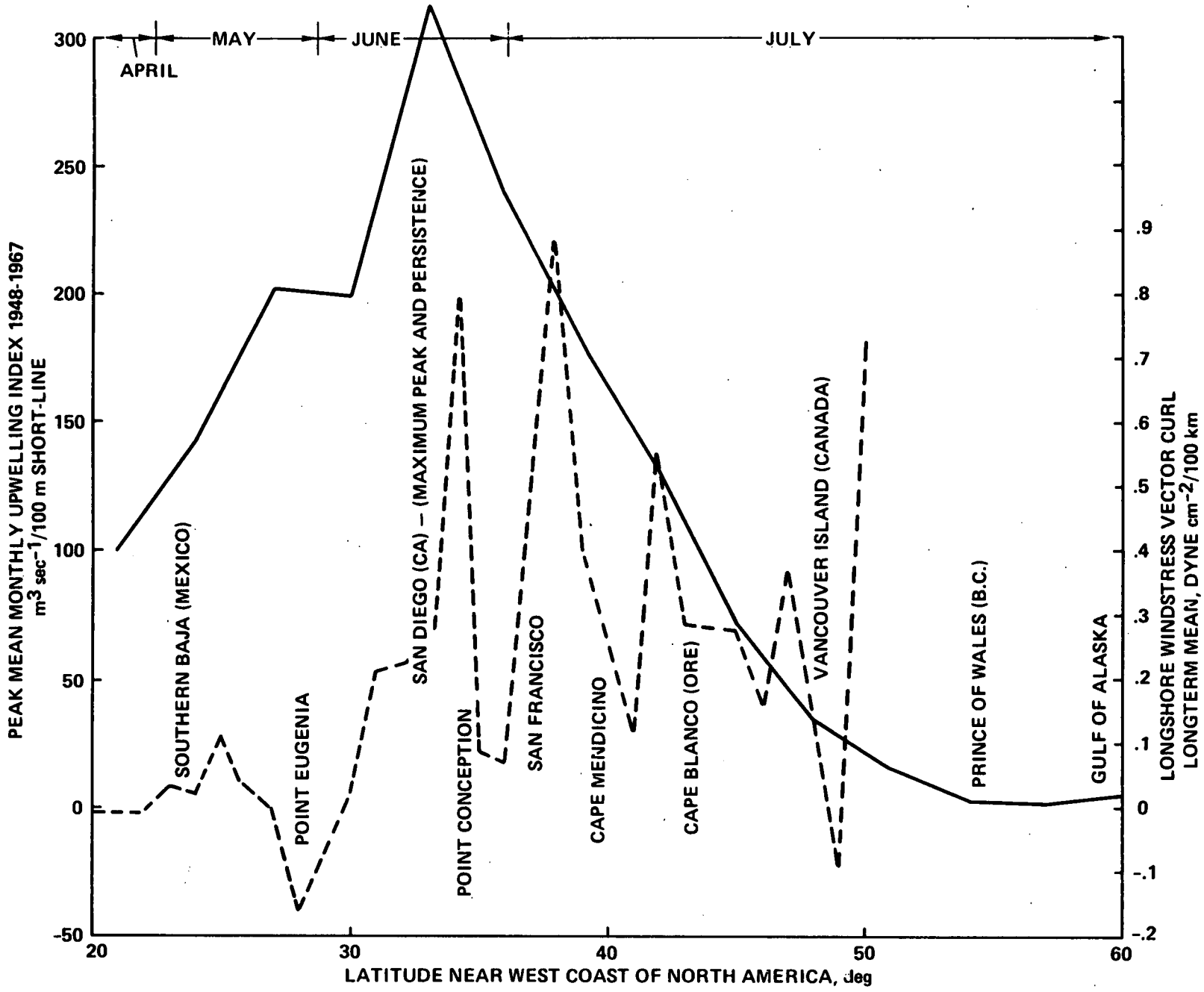

Figure 6.- Latitudinal variation of the long-term mean-monthly upwelling idex peak, and associated wind-stress vector curl.

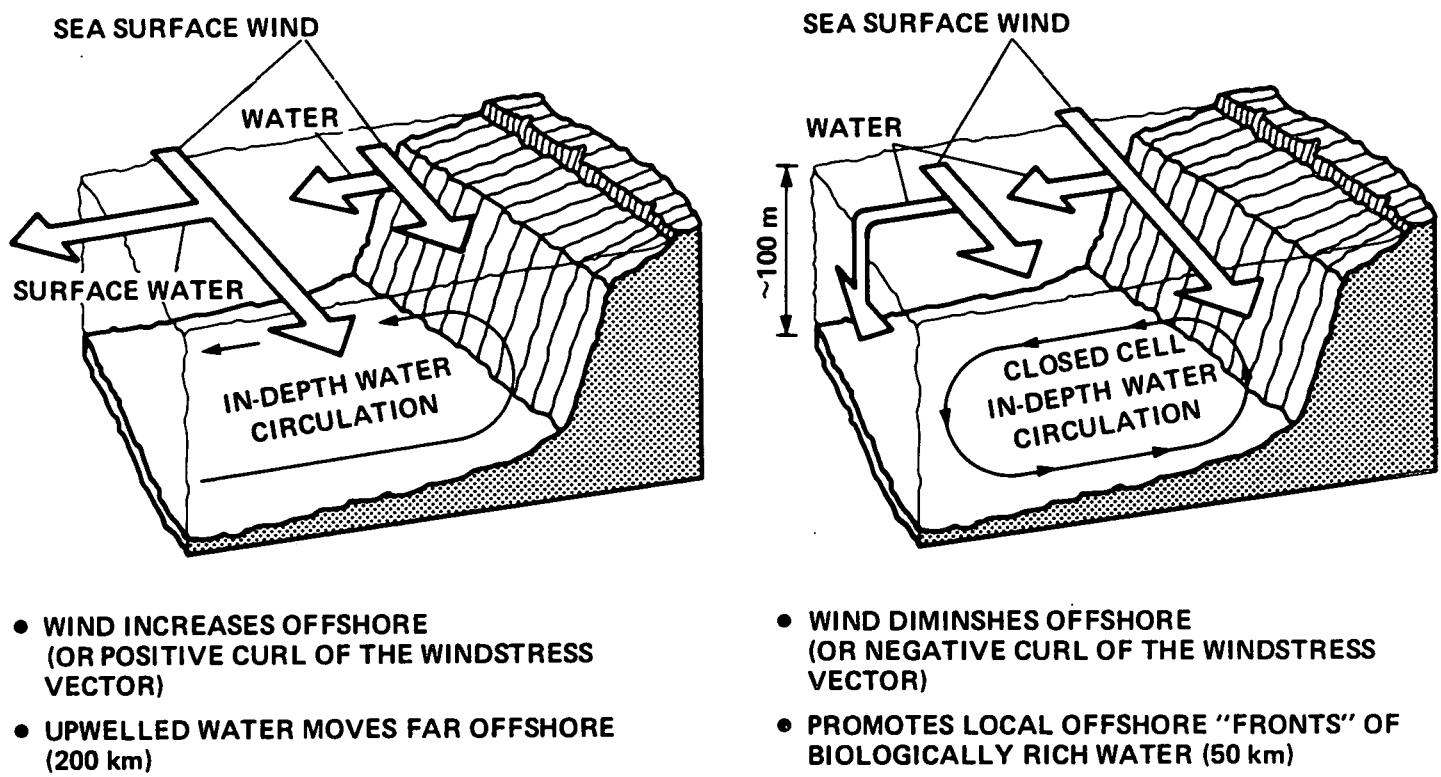

Figure 7.- Effect of the curl of the wind-stress vector on the upwelling structure. (a) Prevailing offshore divergence of upwelled water. (b) Convergent front.

wind diminishes offshore, and a convergent offshore upwelling front tends to form. That is, the upwelling is arrested at the front, downwelling may occur offshore, and (in the simple schematic) a closed cell of recirculated water may develop.

Except near Point Eugenia, Mexico, and locally north of Vancouver Island, Canada, the long-term mean of the curl of the wind stress vector is positive in figure 6, which is conducive to the divergence of upwelled water offshore. It is notable that although the long-term mean values of the curl are small in the region between Point Conception and San Francisco and around the Oregon border, this curl is still positive. Thus the long-term mean condition is conducive to offshore divergence of upwelled water. The two conditions are illustrated in figure 7; figure 7a shows the prevailing offshore divergence of upwelled water, and figure 7b shows the variation which produces a convergent front.

However, we must recall that upwelling occurs in episodes, and during an episode the curl of the wind-stress vector is highly variable and can become negative, so that a convergent offshore front could be formed at some stage of the episode. During the upwelling season, the climate of the west coast of North America is dominated by a high-pressure region offshore, where the wind tends to circulate around that high in a clockwise direction. This high pressure region varies in strength and is not stationary. During a blow, as the high pressure region moves

toward shore, the wind diminishes at sea first and subsequently may cause a negative curl to occur so that at the end of the blow an offshore front is formed. For example, depending on the location of the high, it may move toward the coast so that the wind direction increases from the north and then from the east. Thus, in the San Francisco Bay area, the "typical" springtime marine layer and fog pattern is interrupted and does not move as far inland. The local curl of the upwelling wind-stress vector may become negative temporarily, which promotes the formation of an offshore convergent front. Or, if the wind becomes easterly or southeasterly, the upwelling episode can be arrested entirely. As an observation, Howe (ref. 10) has left port in strong winds, but found that offshore the wind abated (negative curl of the wind stress vector). Near the Farralon Islands, the wind vanished and a convergent offshore front was visible, marked by a line of floating marine organisms as far as the eye could see. Indeed, commercial fishermen have learned to use weather information to help locate such fronts. Thus, if the weather report says that there is strong wind at the San Francisco buoy, and light wind at the Farralon Islands, some people will fish the Farralons because there may be a temporary, but biologically rich, convergent front there. Moreover (ref. 10), on an occasion when strong upwelling in Monterey Bay was terminated by a reversal of the upwelling wind, fish buyers reported that their facilities were strained to capacity one day, and idle the next.

THE EQUATIONS OF CHANGE

It is convenient and useful to relate phenomena that are important to biogeochemical cycling in the sea in mathematical terms through the equations of change. These include the usual equations of motion of oceanography as a subset, as well as equations that describe solar illumination, and a description of chemical and biological events to some level of approximation. We use a left-handed coordinate system x,y,z for convenience in the northern hemisphere with z directed downward. The corresponding water velocities are u, v, and w. The conservation of mass can be written as

$$\frac{\partial \rho}{\partial t} + \frac{\partial(\rho u)}{\partial x} + \frac{\partial(\rho v)}{\partial y} + \frac{\partial(\rho w)}{\partial z} = 0 \tag{1}$$

Similarly, the conservation of momentum in the three coordinate directions is

$$\frac{Du}{Dt} = \frac{\partial u}{\partial t} + u\frac{\partial u}{\partial x} + v\frac{\partial u}{\partial y} + w\frac{\partial u}{\partial z} = 2v\Omega \sin\phi - \frac{1}{\rho}\frac{\partial p}{\partial x} + \frac{1}{\rho}R_x \tag{2}$$

$$\frac{Dv}{Dt} = \frac{\partial v}{\partial t} + u\frac{\partial v}{\partial x} + v\frac{\partial v}{\partial y} + w\frac{\partial v}{\partial z} = -2u\Omega \sin\phi - \frac{1}{\rho}\frac{\partial p}{\partial y} + \frac{1}{\rho}R_y \tag{3}$$

$$\frac{Dw}{Dt} = \frac{\partial w}{\partial t} + u\frac{\partial w}{\partial x} + v\frac{\partial w}{\partial y} + w\frac{\partial w}{\partial z} = -2v_e\,\Omega \sin\phi - \frac{1}{\rho}\frac{\partial p}{\partial z} + g + \frac{1}{\rho}R_z \tag{4}$$

The substantial derivative which appears on the left of equations (2), (3), and (4) contains both acceleration and inertial terms which are expressed as the central equality. On the right-hand equality, the first term is the Coriolis effect of deflection caused by the rotation of the Earth, the central term is the pressure-gradient effect, and the last term contains the viscous effects. The gravity term, g, appears in equation (4) only, which is a statement of the vertical component of forces. The energy equation is

$$\rho c_p \frac{\partial T}{\partial t} + \rho u c_p \frac{\partial T}{\partial x} + \rho v c_p \frac{\partial T}{\partial y} + \rho w c_p \frac{\partial T}{\partial z} = \frac{\partial}{\partial z}\left(k \frac{\partial T}{\partial z} - q_{r_z}\right) \tag{5}$$

where the right side is the vertical energy flux divergence, k is the eddy conductivity, and for the case of absorption, emission, and scattering of radiation on a spectral basis, the divergence of the radiative flux is

$$-\frac{\partial}{\partial z} q_{r_z} = \pi \sum_{\nu=h}^{h'} K_\nu (I_{R_\nu} + I_{T_\nu} - 2n^2 I_{B_\nu}) \tag{6}$$

In this expression, I_{T_ν} and I_{R_ν} correspond to the transmitted and internally backscattered radiative intensity of frequency ν (ref. 11), which are described by a system of two flux equations of radiative transfer (which include emission terms, refs. 11-14).

$$\frac{dI_{T_\nu}}{dz} = -(K_\nu + S_\nu) I_{T_\nu} + S_\nu I_{R_\nu} + K_\nu n^2 I_{B_\nu} \tag{7}$$

$$\frac{dI_{R_\nu}}{dz} = (K_\nu + S_\nu) I_{R_\nu} - S_\nu I_{T_\nu} - K_\nu n^2 I_{B_\nu} \tag{8}$$

Climatalogical conditions provide the boundary conditions at $z = 0$ for equations (2) through (8).

Finally the conservation of each species is stated as

$$\frac{\partial c_i}{\partial t} + u \frac{\partial c_i}{\partial x} + v \frac{\partial c_i}{\partial y} + w \frac{\partial c_i}{\partial z} = J_i + \frac{\omega_i}{\rho} \tag{9}$$

The right side of equation (9) contains the chemical, photochemical, biochemical, and predation processes that relate to the formation or depletion of each specie, i.

Boundary conditions for these equations will be discussed subsequently, where appropriate. In this form, the solution of these equations is not a particularly appealing task. So we now consider important simplifications for specific ocean

applications, and how these may be extended to the present problem. Consider first some simple concepts of ocean currents as derived from approximations of the momentum equations (2), (3), and (4).

OCEAN CURRENTS

Currents Caused by Mass Distribution

Major ocean circulations are governed by the pileup of water in particular regions of the Earth. Correspondingly, the equations of motion are simplified by neglecting friction, the vertical component for the Coriolis term, transient and inertial terms (actually, the entire, substantial derivative (ref. 15); that is, all of the terms to the left of the second equality in equations (2), (3), and (4)). This leads to the hydrostatic equations, where horizontal velocities are related to ocean elevation differences and the rotation of the Earth. (Incidentally, the large gyre that dominates the ocean circulation in the Gulf of Alaska, mentioned in connection with figure 6, could be treated in this manner.)

Wind Driven Ocean Currents and Upwelling

Upwelling has been considered for most of this century to be the result of wind-induced shear stress on the ocean's surface combined with the Coriolis effect of the rotation of the Earth. It is commonly assumed (refs. 16-20) for wind-driven currents, that both the hydrostatic pile up of water and the acceleration terms (actually the entire substantial derivative) can be neglected in the momentum equations (2) and (3). These reduce to a balance of the viscous and Coriolis terms (the first and last terms on the right sides of the equations). The viscous stresses are the product of the eddy viscosity and the gradient of the horizontal velocity with respect to depth.

The resulting equations were originally integrated by Ekman (ref. 16), and subsequently by many others. A discussion of primary features of the upwelling solution appears in reference 18. These solutions of the momentum equations include various approximations and assumptions regarding surface wind stress, shallow- or deep-ocean-bottom boundary conditions, and constant or variable eddy viscosity. Ekman's solution for the deep ocean yields a spiral horizontal velocity variation in which the amplitude is a maximum at the surface and decreases with depth. The result is that surface water is transported at 45° to the right of the wind direction in the northern hemisphere. Importantly, the average motion of the Ekman layer is at a right angle to the wind. This is the conceptual basis for much of the study of upwelling phenomena.

The component of Ekman transport directed offshore, computed for an adjusted geostrophic wind (rotated 15° to the left and reduced 30% by friction), has been termed the upwelling index (refs. 6 and 8). It is an estimate of the transport of surface water offshore. The Ekman mass transport is expressed as

$$\vec{M} = \frac{1}{f} \vec{\tau} \times \vec{k} = \frac{1}{f} \rho_a C_D |\vec{V}| \vec{V} \times \vec{k} \qquad (10)$$

The component directed offshore has the units volume per-second-per-unit length of shoreline. The term f is the Coriolis parameter (a function of latitude), $\vec{\tau}$ is the sea-surface shear-stress vector resulting from the adjusted geostrophic wind, and $\vec{k}$ is a unit vector directed vertically (refs. 6 and 8). The right-hand equality expresses the shear stress in terms of air density, ρ_a, a drag coefficient, C_D, and the adjusted geostrophic wind velocity, $\vec{V}$.

In consideration of the highly idealized simplifications of the momentum equations, the various assumptions employed, and the very irregular boundaries of ocean currents and landmass in nature, we must realize that some of the notions we have about upwelling may be mathematical artifacts, and not physical reality. Although the physics retained in the momentum equations balance the Coriolis term with friction (and other terms by some investigators) (e.g., ref. 21), the Coriolis effect is thought to be important for large-scale ocean circulations, rather than for small ones. Since coastal upwelling is a somewhat spotty phenomenon, it may be surprising that momentum solutions describe upwelling as well as they do. The upwelling index has been used extensively to study the gross features of the transport of coastal waters seaward, and the variation of that transport with latitude and time.

However, for the balance of this paper, it is convenient to abandon this approach. Ekman upwelling described above was originally derived for the deep ocean; for a shallow ocean, Ekman found the surface current to be more aligned with the wind. The shallow ocean (along the continental shelf) and particularly the motion of the thin euphotic layer at the surface (fig. 8) is of biological interest. The coordinate system is aligned with x directed offshore, normal to the coast, y is directed locally parallel to the coast toward the equator, and z is depth measured from the sea's surface. A quasi-steady state is assumed, and any along-shore flow $v(x,y,z)$ is allowed, but $\partial v/\partial y$ is neglected. The continuity equation (1) becomes for incompressible flow

$$\frac{\partial u}{\partial x} + \frac{\partial w}{\partial z} = 0 \qquad (11)$$

Near the shore the solution for upwelling and the offshore movement of water is

$$u = ax \,, \qquad w = -az \qquad (12)$$

respectively. Similarly, if a convergent front exists offshore at $x = \delta$, the solution of equation (11) in that vicinity will be shown to be of the form

$$u = b(\delta - x) \,, \qquad w = bz \qquad (13)$$

For generality, wind speed and direction just offshore can be adjusted arbitrarily to account for the frictional boundary layer, and Coriolis or other effects; hence, the surface velocity and its components in the surface layer of the ocean where photosynthesis occurs, is taken to be proportional to the local adjusted wind velocity and its components (the right side of fig. 8).

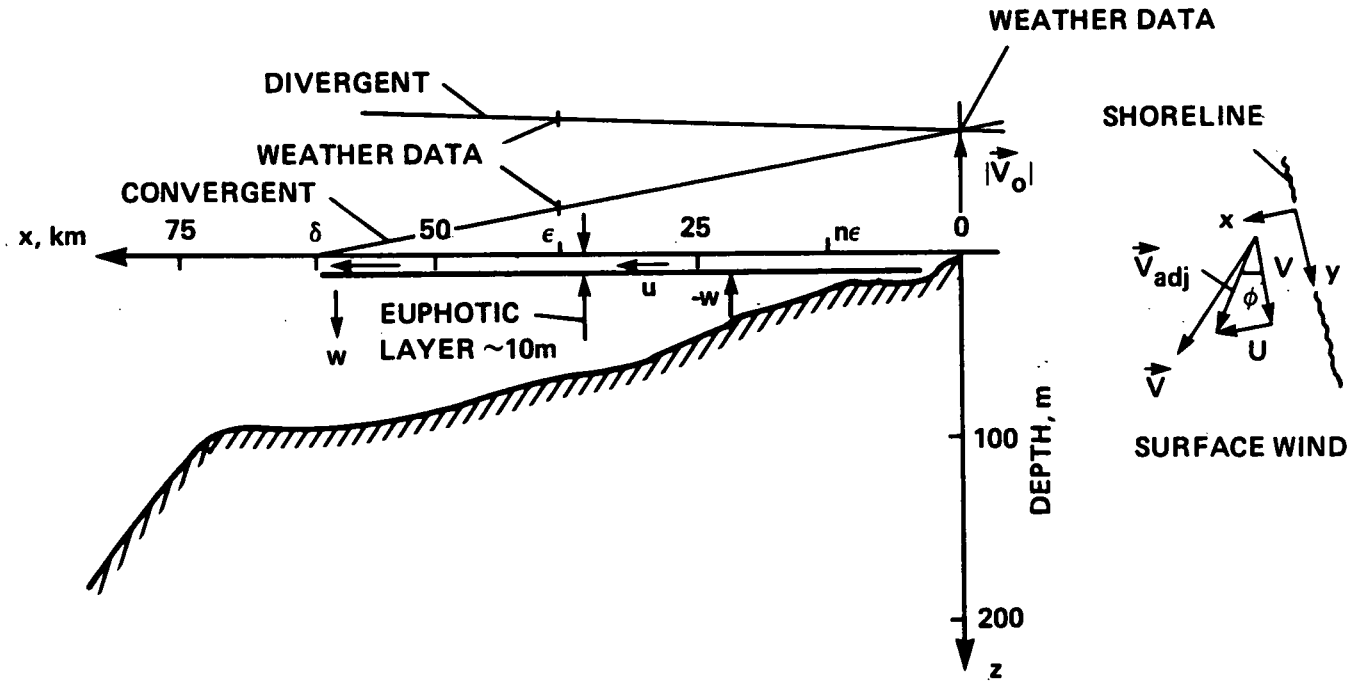

Figure 8.- Upwelling/wind schematic, bathymetry ~37° 50' n.

The adjusted wind is taken to be a linear function of the distance from shore;

$$\vec{V}_{adj} = \vec{V}_0(1 + mx) \tag{14}$$

Consider that real-time weather data exist near shore, and at a distance of ε offshore. At a distance $x \geq n\varepsilon$ (where n is a fraction) the components of the wind velocity are

$$U(x) = U_0(1 + mx) , \qquad V(x) = V_0(1 + mx) \tag{15}$$

where it may be noted that the curl of the component of the wind vector parallel to the coast is

$$\frac{\partial V}{\partial x} = mV_0 \tag{16}$$

The surface velocity of the water in the x-direction is

$$u(x) = cU = cU_0(1 + mx) , \qquad x \geq n\varepsilon \tag{17}$$

That relation can be derived readily for the laminar flow of wind blowing over water by matching shear stress at the water/air interface between boundary layers in the air and water. The proportionally constant, c, is essentially the cube root of the ratio of the density viscosity product in the air, to that in the water. It varies from 0.025 to 0.03 for surface temperatures between 10°C and 20°C. For turbulent wind/ocean conditions, a simple proportionality can be argued; the constant 0.035 has been used in the U.S. Geological Survey (USGS) oilspill trajectory model (ref. 22).

At $x = n\varepsilon$, the velocity given by equations (12) and (17) are equal and

$$u(n\varepsilon) = cU_0(1 + mn\varepsilon) = an\varepsilon \tag{18}$$

Thus the coefficient, a, is determined to be

$$a = \frac{cU_0}{n\varepsilon} = cU_0 m\left(1 + \frac{1}{mn\varepsilon}\right) \tag{19}$$

where n will be determined subsequently. Thus for a given wind condition, the motion of the surface waters and the curl of the wind vector can be approximated simply for present purposes.

It may be noted in figure 8 that the horizontal scale is greatly foreshortened. The bathymetric profile shown crosses the Gulf of the Farallones at latitude ~37°50'N. The ocean floor is a broad area that slopes gently to the edge of the continental shelf. A significant feature is that the depth is not excessive ($\leq$100 m). In principle, bottom waters and nutrient rich sediments can be upwelled to the sunlit surface over much of the region.

SOLAR RADIATION IN THE SEA

The absorption of sunlight in the surface layers of the ocean is of primary importance to biogeochemical events. Most of the ocean is essentially a wet desert, with the exception of limited regions wherein nutrients are exposed to sunlight in surface layers where they participate in the production of a biomass. Thus regions of coastal upwelling are of major importance to the biogeochemistry of the Earth.

Three features of the sea surface must be mentioned as background to what follows. First, although the upwelling may arise from depths of the order of 100 m, the euphotic zone where sunlight interacts with organic matter is much more shallow--of the order of 10 m. It is estimated that 90% of all sunlight is absorbed in the upper 10 m of the sea (refs. 23 and 24). Coastal water absorption in the blue, green, yellow, and orange parts of the spectrum is two or three times that in

oceanic water, and infrared absorption occurs at the surface. Secchi disc observations made by the author in 150 m depths off Point Sal, California, showed that the white Secchi disc could not be seen at depths greater than approximately 4 m. Importantly, light at a wavelength of 450 nm that is absorbed by chlorophyll pigments in phytoplanckton has an extinction coefficient of about 1 m^{-1}, and is diminished by 90% at a depth of less than 2.5 m.

Second, it should be noted that for an ordinary "random" sea of 2 m or so, the superficial euphotic layer may be considered to be well-mixed.

Third, the sinking rate of phytoplanckton is exceedingly small in the euphotic zone. This can be estimated by forming the ratio of the depth, z, where light with a wavelength of 450 nm is attenuated by a factor $q_{r_\nu}/q_{r_{\nu_0}}$ to the settling velocity of a biomass particle of size d. The resulting residence time is

$$t = \frac{1}{K_\nu} \ln\left(\frac{q_{r_{\nu_0}}}{q_{r_\nu}}\right) \times \frac{18\mu}{d^2\rho(\rho_m/\rho - 1)g} \tag{20}$$

where in this expression only, K_ν refers to the physical absorption coefficient and not to the Kubelka-Munk absorption coefficient (a factor of 2 different). For biologically rich coastal waters where K_ν is of the order of 1 m, the residence ime required for a particle to sink to a depth where light is attenuated by 90%, is of the order of 100 yr to 10 yr for small particles of 5 μm- to 20 μm-diam. For larger particles or clusters of 100-μm size, the residence time is half a year. For these particles, the biomass is diminished by predation, starvation, disease, old age, or ocean currents; but not by sinking. For large particles or clusters of millimeter size, the residence time in euphotic coastal waters is of the order of a day. In clearer oceanic water where light absorption is weak, the residence time is increased by a factor $1/K_\nu$ (as much as the order of 10).

Thus for assessing the effect of sunlight on the sea, we need only to consider a superficial layer in which phytoplanckton has a long residence time, which has a thickness of less than 10 m, and which is well-mixed. This is a useful and important simplification. With that in mind, let us turn to the energy equation (5), the equation for the radiative flux divergence (6), and the differential equations of radiative transfer in a scattering, absorbing, and emitting medium (eqs. (7) and (8)).

For purposes of energy considerations, absorption is large when compared with scattering ($K_\nu >> S_\nu$) for phytoplanckton. Thus the scattering coefficient, S_ν, and the backscattered intensity, I_ν, can be neglected (of course neither can be neglected for remote sensing signal analysis--a related problem that is readily treated). Radiant emission at 450 nm can be neglected, and the radiant intensity of photons of frequency, ν, in the z direction at a depth z can be obtained from equation (7) and is

$$I_{T_\nu} = \frac{q_{r_{\nu_0}}}{\pi} (1 - \rho_{s_\nu}) e^{-K_\nu z} \tag{21}$$

where ρ_{s_ν} is the surface reflection coefficient for photons of frequency, ν, incident on the ocean. Correspondingly, the divergence of the incident flux $q_{r_{z_\nu}}$ at depth z is from equations (21) and (6)

$$-\frac{\partial}{\partial z} q_{r_{z_\nu}} = q_{r_{\nu_0}} K_\nu (1 - \rho_{s_\nu}) e^{-K_\nu z} \tag{22}$$

If we sum the contributions over all frequencies, and average the radiation absorbed by integrating across the euphotic layer of thickness, d_e, we obtain

$$-\frac{\partial}{\partial z} q_{r_z} = \sum_{\nu=0}^{\infty} \frac{q_{r_{\nu_0}} K_\nu (1 - \rho_{s_\nu})}{d_e} \int_0^{d_e} e^{-K_\nu z} \, dz \tag{23}$$

For the quasi-steady state in a well-mixed layer where temperature varies slowly in the z and y directions, the energy equation (5) combined with equation (23) yields

$$\rho u c_p \frac{\partial T}{\partial x} = \frac{1}{d_e} \sum_{\nu=0}^{\infty} q_{r_{\nu_0}} (1 - \rho_{s_\nu})(e^{-\mu_\nu d_e} - 1) \tag{24}$$

whose solution describes the temperature variation in the euphotic layer as a function of the distance from the shoreline. Both the temperature variation and light intensity are important because these affect the rates at which reactions proceed. The growth rate of phytoplankton diminishes with decreased temperature (ref. 25), and the rate of metabolism of ocean organisms is approximately doubled by a 10°C increase in temperature (ref. 26).

For convenience, define

$$Q_r \equiv \frac{1}{\rho c_p d_e} \sum_{\nu=0}^{\infty} q_{r_{\nu_0}} (1 - \rho_{s_\nu})(1 - e^{-\mu_\nu d_e}) \tag{25}$$

and if i is a small distance from shore where the temperature T_0 is known,

$$x \equiv i\bar{x}, \qquad dx = i \, d\bar{x} \tag{26}$$

Equation (24) can be written

$$\frac{T}{Q_r} = \int \frac{d\bar{x}}{iu} + \text{constant} \tag{27}$$

With reference to figure 8, equation (27) can be integrated to obtain

$$\left(\frac{T - T_0}{Q_r}\right) = \frac{1}{a} \ln \frac{x}{i} , \qquad x \leq n\varepsilon \tag{28}$$

Similarly, from weather data at $x = \varepsilon$

$$\left(\frac{T_\varepsilon - T}{Q_r}\right) = \frac{1}{cU_0 m} \ln \left(\frac{1 + m\varepsilon}{1 + mx}\right) , \qquad x \geq n\varepsilon \tag{29}$$

At $x = n\varepsilon$, the temperature is continuous so that from equations (28) and (29),

$$\left(\frac{T_\varepsilon - T_0}{Q_r}\right) cU_0 m = \ln \left(\frac{1 + m\varepsilon}{1 + mn\varepsilon}\right) + \left(\frac{mn\varepsilon}{1 + mn\varepsilon}\right) \ln \frac{n\varepsilon}{i} \tag{30}$$

This is the transcendental compatibility equation whose solution is n, the match point in surface velocity which is shown in figure 8 and mentioned in connection with equation (15).

For the case of a convergent front offshore at $x = \delta$, δ can be taken to be the known weather data location (by extrapolation if necessary). Thus for convenience, $\delta = \varepsilon$ and $m = -1/\delta$ so that in the vicinity of the front

$$u = cU_0 \left(1 - \frac{x}{\delta}\right) = \frac{cU_0}{\delta} (\delta - x) = b(\delta = x) \tag{31}$$

which defines b and is of the form of equation (13) as mentioned previously. However, as the front is approached, $x \to \delta$, and $T_\delta \to \infty$; this is an unpleasant mathematical artifact. So let us say that at $x = (\delta - i)$, $T \simeq T_\delta$ in equation (10) which affects the first term of the right-hand side of the compatibility of equation (30). Thus for offshore convergence, the compatibility relation can be put in the form

$$\left(\frac{T_\delta - T_0}{Q_r}\right) \frac{cU_0}{\delta} = \ln \bar{\delta}(1 - n) + \frac{n}{n - 1} \ln n\bar{\delta} \tag{32}$$

where

$$\bar{\delta} = \frac{\delta}{i} >> 1 \tag{33}$$

Correspondingly, equation (27) can be integrated to yield

$$\left(\frac{T - T_0}{Q_r}\right)\frac{cU_0}{\delta} = \left(\frac{T_\delta - T_0}{Q_r}\right)\frac{cU_0}{\delta} - \ell n\ \bar{\delta}\left[\left(1 - \frac{x}{\delta}\right)\right], \qquad \frac{x}{\delta} \geq n \tag{34}$$

For offshore convergence, the compatibility relation for n is plotted as a family of curves in figure 9, and is illustrated as follows. For a day of average cloudiness along the west coast in July (ref. 27), the left side of equation (32) can be estimated in a straightforward way. The summation, Q in equation (25) may be 0.027 W/cm^2 averaged over a 24-hr day. (It may be higher than that during a blow when no cloud cover is present, and lower as the blow diminishes and the cloud cover increases.)

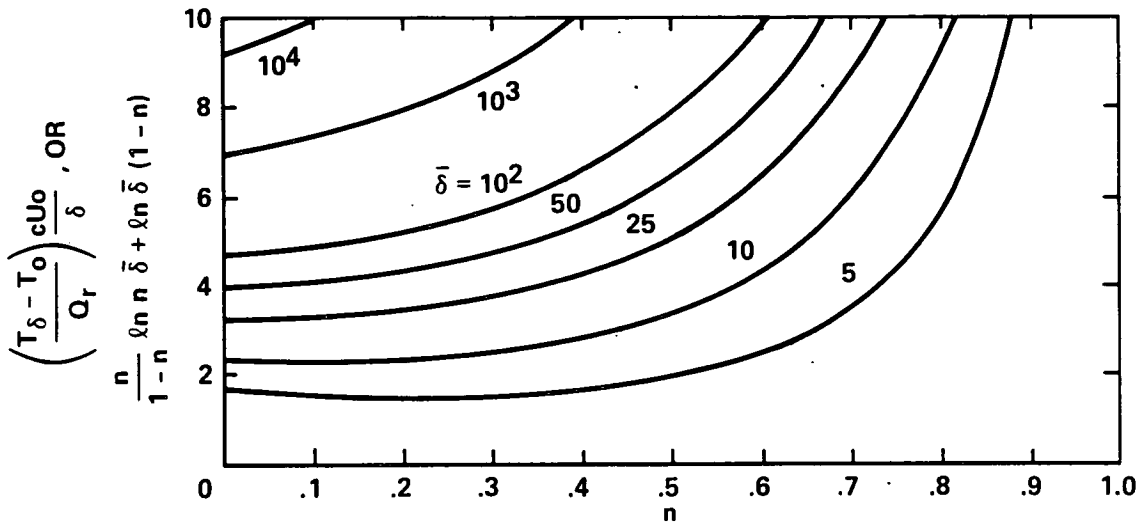

Figure 9.- Match point location (eq. (32)).

Assume that d_e = 10 m, $T_\delta - T_0$ is 4 K, U_0 is 10 m/sec (a blow), and δ is approximately 50 km. The left side becomes 4.33. If T_0 is known at i = 1 km, $\bar{\delta}$ is 50, and n is found to be 0.22 from figure 9. the corresponding temperature in the euphotic layer is shown in figure 10 as a function of distance offshore.

It may be noted in figure 10 that the temperature rises sharply near shore where the surface velocity (eq. 12) is small, so that the residence time for heating is enhanced. Similarly, near the front ($\bar{\delta}$ = 50 for this example), the surface velocity diminishes to zero (eq. (18)), and both residence time and temperature are enhanced. The inset in figure 10 is a NOAA sea surface thermal analysis plot for July 1984. It shows surface isotherms that appear to converge near the frontal location off Point Arena. As mentioned above in figure 6, such fronts have been observed by the author south of that region under these approximate conditions. The raw temperature data shown are from 10°C at $\bar{x}$ = 1 to 13°C behind the front. The 14°C symbol at x/δ = 1.16 actually corresponds to the first isotherm west (left) of the front.

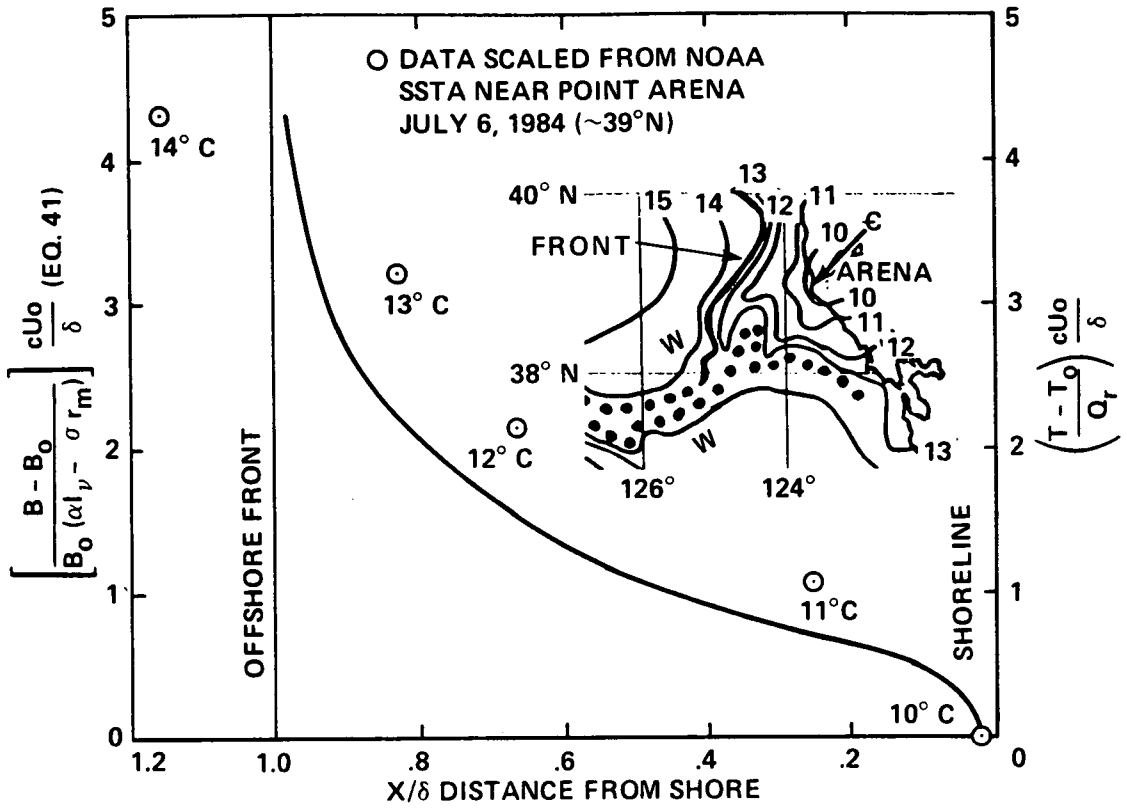

Figure 10.- Surface temperature/(biomass) variation; $\bar{\delta}$ = 50, δ = 50 km, n = 0.22.

This straightforward treatment of the energy and radiative transfer equations (5)-(8), combined with the continuity equation (1), provides usable results for sea surface layer considerations. A more elegant solution of the energy equation (5), in which only the partial derivatives with respect to t and y were neglected, was obtained in the form of confluent hypergeometric functions by Howe (ref. 10). However, the result was more bother than it was worth. A further simplification by the author in which the second partial derivative with respect to z is neglected (the first derivative is retained) has also led to a solution of the energy equation. Although it is more tractable than that of reference 10, it is not yet particularly illuminating, and awaits further consideration.

Before proceeding, it should be noted once again that our considerations are qualitative estimates; that climate and ocean phenomena vary from moment to moment, with latitude and shoreline topography; and that established upwelling patterns are altered by weather change and by the sluggish California current that moves irregularly offshore toward the equator.

BIOLOGICAL AND CHEMICAL CONSIDERATIONS

In the overall biogeochemical cycle in the sea, chemical nutrients and sunlight produce plant blooms in surface waters which in turn support animal life from protozoa to the higher forms. Both plants and animals ultimately die, and they and animal excreta sink and are decomposed by bacteria to form minerals which are upwelled in sunlit waters during that season of the year, and thus continue the intermittent cycle. Some features of the overall process are shown schematically (highly simplified) in figure 11, which is an attempt to illustrate concepts described in references 26 and 28. Oceanic and boundary current waters with their biochemical content contribute to this simple picture. In this section, we will attempt to illustrate some aspects of this cycle--both by exhibiting some biomass observations and by obtaining an idealized, well-behaved solution to a biomass equation.

Figure 5 showed the satellite image of upwelled water along the central California coast on April 13, 1981--the result of strong northwesternly winds shown in figure 4. The latter figure showed the thermal response of the ocean to the wind episodes that gave rise to upwelling characterized by an upwelling index near the 20-yr-mean-monthly peak near Point Sal (the solid symbol in fig. 3).

In situ biological estimates were made by the author near Point Sal on April 13, 1981. A secchi disk and a correlation of NASA and NOAA data (Nolton, ref. 29) were used to estimate chlorophyll concentration. The results appear as the three solid square symbols in figure 12. Of the observations taken four times during the day, two were identical, so the three symbols represent four observations. The concentrations obtained are at the high end of the data base for the correlation, approximately 10 mg/m^3.

Two to four weeks earlier, airborne remote sensing data (ref. 30) in the Point Sal region showed low chlorophyll concentrations--2% to 5% of those shown above. Wind conditions obtained by the aircraft at an altitude of 500 ft varied greatly in strength and direction during that time, with southerly winds March 18 and 20 being conducive to onshore downwelling and followed by northwesterlies March 22-24 and 27-30. No biological interpretation was given. Clearly, extensive water sampling should be obtained at meaningful times and at locations in the upwelling system to enhance understanding of biological phenomena, and to calibrate both surface and remote sensing observations.

With respect to predation on the surface biomass, daytime shipboard echosounder traces on station near Point Sal on April 13, 1981, show zooplankton near the ocean floor (trace B, fig. 13). The bottom of the ocean is shown by the dark outline at the lower part of the traces, above which the water column is shown from approximately 80 m to 150 m below the surface. Dark masses in the water column are schools of fish. Identification was by the captain of the vessel--a veteran fisherman who was able to predict the content of the net (quantity and species) before the net was brought aboard. Near the bottom, gray areas are noted as shortbelly, shrimp, plankton, and krill; rock cod and hake are noted on the trace, and from

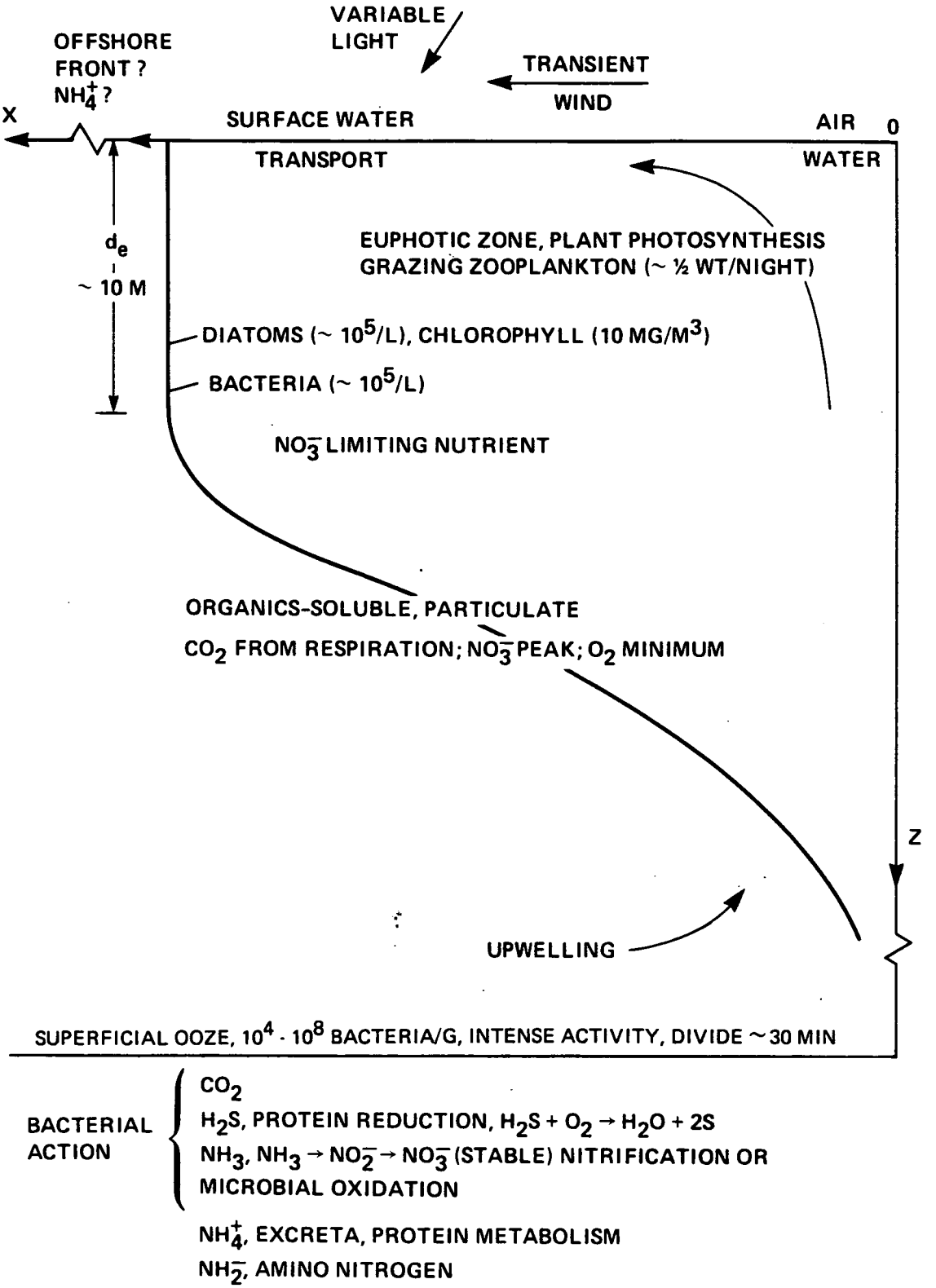

Figure 11.- Biogeochemical cycling diagram of the upwelling water column.

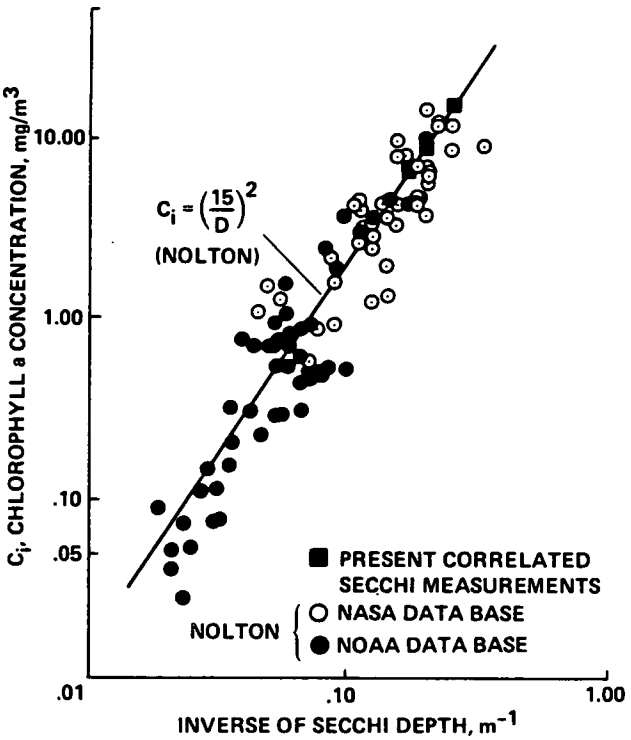

Figure 12.- Chlorophyll-Secchi data and correlation, present Secchi measurements.

approximately 100 m to 150 m, hake and sablefish are shown. In other portions of the record that are not shown, schools of young hake were found close to the bottom.

The plankton shown are not the surface phytoplankton; rather, these are zooplankton, which consist of small crustaceans, jellyfish, worms, mollusks, eggs, and other larval stages. These animals consist of floaters and weak swimmers, which are characterized by diurnal vertical motion. At night, such a trace would show them to be near the surface, supposedly grazing on the phytoplankton. In the morning, these small creatures return to the bottom and in turn are grazed upon by bottom dwellers. Around sunset, the zooplankton mass begins to rise at a rate approaching 7 m/min (ref. 31), so that the migration is complete by 10 to 11 p.m. This appears to be the mechanism whereby bottom fish are nourished by a surface phytoplankton bloom caused by the upwelling of nutrients into surface layers where photosynthesis supplies the needed energy.

The water column in the upwelling regions of the continental shelf (fig. 11) may be considered as a surface layer and a bottom layer of intense biological activity. That is, the euphotic layer at the surface is dominated by the photosynthetic production of phytoplankton in the spring and summer. The bottom is dominated by intense bacterial activity in a thin layer of detrius where organic matter is converted into minerals. In between those two layers, a mixture of chemical and biological phenomena proceed with far less intensity. Thus for convenience, we may perhaps spatially separate the water column to capture the main feature of

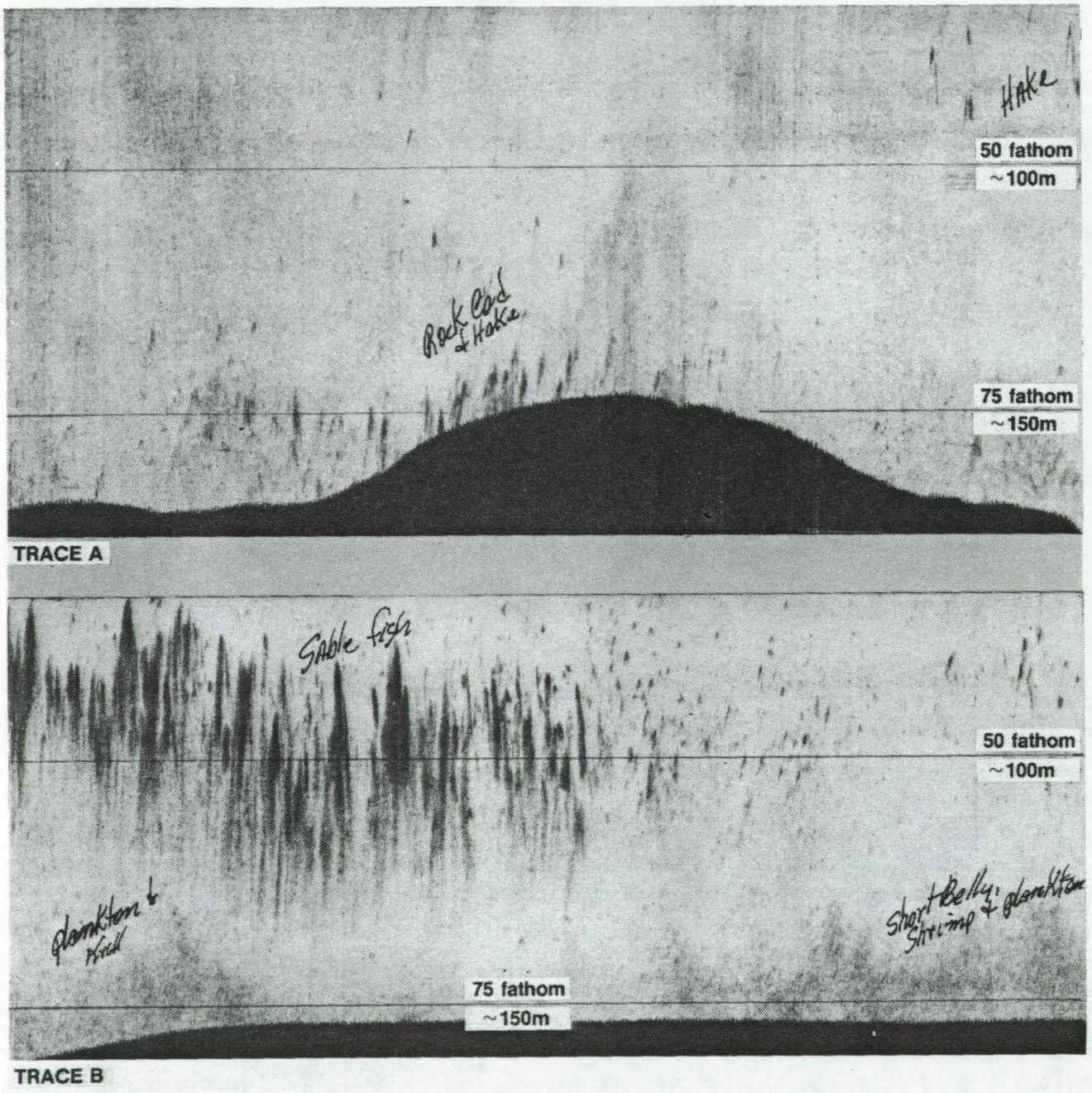

Figure 13.- Typical echo-sounder traces in lower part of water column with species noted.

biogeochemical cycling. Moreover, if the formation of chemical species near the bottom occurs to a large extent in the fall and winter, it may be possible to separate future considerations temporally as well. Thus concentrations of nutrients may accumulate near the bottom during part of the year, and may be upwelled subsequently to the surface, to participate in the phytoplankton bloom. The spatial and temporal

simplification of biological and chemical events would facilitate analysis of the system, but it remains to be seen whether or not such an approach is realistic.

The microbiology of the bottom is exceedingly complex by itself. Indeed, it may not be described in rigorous detail in the near future. Perhaps it does not have to be (after millennia in the fire age, we still cannot show how carbon monoxide is oxidized--but fire is necessary and useful to civilization). Bottom water sampling of an ocean region of interest over a period of time can probably tell us all that is necessary to understand and model the system. The same is true of mid-water and surface water sampling.

With reference to figure 11, bacterial activity is apparently high near the ocean's surface, diminishes with depth, and then it increases enormously in the bottom ooze. A result of bacterial decomposition of matter is that ammonia, carbon dioxide, and hydrogen sulfide are formed. Nitrification or microbial oxidation of ammonia to form nitrite and nitrate is an exceedingly important process. The nitrogen cycle in the sea is complicated and has multiple pathways. Nitrite and ammonium may be only transient intermediate species in the production of the thermodynamically stable nitrate. The nitrate is the second most abundant nitrogen species overall, and with chlorophyll, the nitrate plays primary roles in surface productivity. The peak nitrate concentration occurs below the euphotic zone where oxygen concentration is a minimum. The most abundant nitrogen species is N_2 which is near saturation levels but which is generally inert. Nitrogen also appears dissolved in the amino form NH_2^-, in nitrous oxide, and in particulate nitrogen-bearing substances. During the winter months the surface concentration of nitrate reaches a peak, which is exhausted during the upwelling season when surface blooms of phytoplankton occur. Chlorophyll is the nitrogenous component of particulate material which absorbs light at 450 nm. Although chlorophyll concentration is generally a fraction of a microgram per liter in the open ocean, it may be as high as 40 µg/ℓ in biologically rich coastal upwelled water where it is of primary importance to productivity. Importantly, chlorophyll can be sensed remotely or in situ (by various methods), and nitrate can be obtained by in situ samples which can be analyzed in the laboratory with little deterioration because of its stability.

Carbon dioxide is dissolved in the water from the atmosphere, and is produced by the respiration of all organisms. The bulk of the carbon may come from skeletal remains decomposed by bacterial action. Sulfur is biologically important; its concentration appears to be a maximum in the bottom ooze as part of the microbial decomposition process. It may be detected at low tide when the aroma of H_2S is noticeable.

The above are qualitative notions about the biochemical phenomena involved in coastal upwelling. All of the details of these events are not yet known, and it is not possible to generalize the treatment of the problem from one region to another. Nevertheless the purposes of this introductory paper are served in the sense that a framework is provided in which to study and integrate these many climatological, oceanographic, biological, physical, and chemical events, processes, and observations.

For present purposes, it may be of some interest to form an idea of the gross behavior of the upwelling system under idealized conditions, quasi-steady, not nutrient-limited, and with "smoothly varying" predation. Several attempts have been made to model the phytoplankton biomass mathematically as it grows in nourished sunlit surface layers and as it is diminished by predation. A model developed by Denman and Platt (ref. 32) is

$$\frac{\partial B}{\partial t} + \vec{u} \cdot \nabla_H B + w \frac{\partial B}{\partial z} = D_H \nabla_H^2 B + D_V \frac{\partial^2 B}{\partial z^2} + P_m^B \cdot B \tanh \left[\frac{\alpha I_z(z)}{P_m^B} \right] - r_m [1 - e^{-\sigma(B-\underline{B})}] \tag{35}$$

which can be shown to be of the form of the species of equation (9). Here $\vec{u}$ and w are mean horizontal and vertical velocities, D_H and D_V are horizontal and vertical diffusion coefficients, the next to the last term is the species production rate as affected by light intensity $I_z(z)$, and the last term accounts for predation. Almost any mathematician who goes to sea, as the upwelling wind episode subsides enough to allow that venture, quickly loses interest in vertical derivatives, and second derivatives of any kind for first estimates in surface layers. Indeed, during the upwelling season, the swell is generally from a southerly direction (a result of storms in Antarctica), and the wind-driven sea is generally from a northerly direction. The consequences are a generally confused sea surface and considerable mixing in the upper layers. Thus for the quasi-steady state, and for locally well-mixed surface water where along-shore derivatives are negligible, equation (35) reduces to

$$u \frac{dB}{dx} = P_m^B B \tanh \left(\frac{\alpha \bar{I}_\nu}{P_m^B} \right) - r_m (1 - e^{-\sigma B}) \tag{36}$$

where for convenience, $\underline{B}$ has been set to zero, and $I_z(z)$ has been replaced with $\bar{I}_\nu$. The latter is the radiative intensity of frequency, ν, which is considered to be completely absorbed in the well-mixed euphotic layer. It is thus the unreflected portion of the incident photons of frequency which takes part in photosynthesis.

Further assumptions are made to derive a simple solution to equation (36) so that a baseline idea of how the upwelling biosystem behaves under favorable circumstances can be obtained. These assumptions may, of course, be relaxed in a more detailed study. Thus for present purposes, if

$$\left| \frac{a^2}{3} \right| \ll 1 , \qquad \tanh a \approx a \tag{37}$$

and if

$$\left|\frac{a^2}{2!}\right| \ll 1 , \quad e^{-a^2} \approx 1 - a^2 \tag{38}$$

Under these conditions, equation (36) becomes

$$u \frac{dB}{dx} = B\alpha\bar{I}_\nu - r_m\sigma B \tag{39}$$

The solution yields the phytoplankton biomass variation as a function of distance offshore;

$$B(x) = B_0 \, e^{(\alpha\bar{I}_\nu - r_m\sigma) \int_i^x dx/u} \tag{40}$$

Again if the exponent of the exponential is sufficiently small, this becomes

$$\frac{B(x) - B_0}{B_0(\alpha\bar{I}_\nu - r_m\sigma)} = \int_1^{\bar{x}} \frac{d\bar{x}}{iu} \tag{41}$$

which is the same form as equation (27). (It may be noted that the integral in the exponential in eq. (40) is the time required to move surface waters offshore from x = i. Thus, for large x, the exponential may be sufficiently large that eq. (40) is more appropriate than eq. (41).)

The solution of equation (41) for offshore divergence is identical to equations (28) and (29) with the left side of equation (41) replacing those of equations (28) and (29), appropriately.

The solution of equation (41) for offshore convergence is the same as it is for equations (32) and (34) with similar replacements, and is shown in figure 10 with the left ordinate labeled as shown.

The result for both the divergent and convergent cases is that the biomass concentration variation is identical to the surface temperature variation. Thus for this idealized baseline case, the biomass concentration variation could be sensed with a thermometer or estimated from NOAA sea surface thermal analysis biweekly charts.

Of course, upwelling is not an idealized phenomenon. There are several factors which are implicit in equation (41): (1) sufficient nutrient availability is indicated; (2) spatial variation of predation is negligible; (3) steady state is assumed; (4) there is no intrusion of biologically poor oceanic water; and (5) there is an absence of other unpleasant influences. Biomass concentration variations are often irregular and are contrary to expectation for reasons which need to be

understood. But we have a notion of what upwelling could produce biologically, and a reinforced conviction that remote and in situ observations, laboratory studies, and further analysis which relate to these features are essential to monitoring and understanding the entire interrelated upwelling/biological system.

CONCLUDING REMARKS

Major spatial and temporal features of coastal upwelling along the west coast of North America have been presented and discussed. Some local biological and physical information obtained by buoy data and in situ observations which include the entire water column have been presented as well as large scale data obtained by satellite and aircraft remote sensing. Features of the overall biogeochemical cycling system as affected by coastal upwelling have been outlined and where possible, have been related to the observations. Discrepancies have been cited and the need for information that will enhance the understanding of the processes that affect the cycling of chemical species in the waters along the continental shelf has been noted. Knowledge of both the features of the cycling phenomena and the rates at which they change needs to be enhanced.

The relationships of weather, oceanography, biology, chemistry, light, and physics have been formulated deterministically. This formulation provides a convenient framework for performing research, a means for ranking the importance of specific biogeochemical features (by ordering and by comparing terms in the equations of change), and as a means of identifying basic information that is needed to solve the cycling problem to any level of detail that is desired. As a first approximation, the main features of biogeochemical cycling in upwelling systems may be divided spatially into two parts for convenience: ocean surface phenomena which include the phytoplankton bloom, and ocean floor phenomena which include the microbial conversion of organic material to minerals. It may be possible to further divide the problem temporarily, the link in time being the onset of upwelling which brings bottom nutrients into the thin surface euphotic zone.

A preliminary illustrative result for ocean surface layers has been obtained which includes the effects of weather, oceanography, dynamics, energetics, light, biomass production, and predation for a "well-behaved" biogeochemical cycling system in upwelling. The result has been compared with sea-surface tghermal-analysis observations near the California coast. A biomass-temperature analogy for this well-behaved system was shown. The analysis could be perturbed for irregular or "poorly behaved" effects. It was noted that the equations which describe light scattering and absorption in the sea can be solved quite readily relevant to remote sensing signals. Future research activities were identified. Weather data for selective locations should include information concerning the spatial and temporal variation of surface wind shear stress, the curl of the wind stress vector, and both incident and backscattered light intensity on a spectral basis. Oceanographically, selective surface water sampling and analysis should be obtained and related to the progressicn of upwelling events. Transient phenomena and offshore frontal formation

data should be acquired and related to the behavior of the system. Biologically, the spatial and temporal variation of bottom activity should be examined by selective sampling of bottom water and sediments to sort out the dominant features of chemical and microbiological reactions and their rates as they are affected by the behavior of the overall upwelling system. With respect to remote sensing, spectral scattering in water by plankton and other particulates should be characterized. The effect of the atmosphere and the air/sea interaction on light scattering and attenuation should be examined more thoroughly. Corresponding solutions to the Kubelka-Munk equations of light transfer through densely distributed scattering sites should be obtained. Computationally, the modeling of biogeochemical phenomena should be improved. Transient and three-dimensional effects should be examined. A bottom flow analysis should be developed which includes the conversion of organic to inorganic species.

In the long term, solutions to the entire set of the equations of change over the entire domain, including rich physical and biological detail, the proper rate and property inputs, and the appropriate boundary condition (including climatological variations) should be able to describe the state of the entire biogeochemical cycling system, and could be used predictively to estimate the future course of events. As techniques improve they have potential application to other upwellings: along the west coasts of Africa and South America, Polar ice shelves, and boundary currents of major offshore ocean circulations. It may be that the redeeming feature of biogeochemical cycling in the vast ocean is that dominant events tend to be rather localized.

REFERENCES

1. Daghir, E. P.: Sea Surface Thermal Analysis. National Weather Service, National Oceanographic and Atmospheric Administration, San Francisco, CA, 1984.

2. Anon.: Sea Surface Temperature °F. National Marine Fisheries Service, National Oceanographic and Atmospheric Administration, LaJolla, CA, 1975.

3. Daghir, E. P.: National Weather Service. Computer-Enhanced-Infrared Satellite Image, National Oceanographic and Atmospheric Administration report, 1984.

4. Anon.: The Fish Boat, H. L. Peace Publications, Covington, LA, Oct. 1985, p. 13.

5. Ryther, J. H.: Photosynthesis and Fish Production in the Sea. Science, vol. 166, 1969, pp. 71-76.

6. Bakhun, A.: Coastal Upwelling Indices, West Coast of North America 1946-1971. NOAA Tech. Rep. NMFS-SSRF-671, 1973.

7. Howe, J. T.; Gibson, D. B.; Evans, T. O.; Breaker, L.; Wrigley, R. C.; and Broenkow, W. W.: Biological and Physical Oceanographic Observations Pertaining to the Trawl Fishery in a Region of Persistent Coastal Upwelling. NASA TM 81332, 1981.

8. Bakhun, A.: Daily and Weekly Upwelling Indices, West Coast of North America 1967-1973. NOAA Tech. Rep. NMFS-SSRF-693, 1975.

9. Nelson, C. S.: Wind Stress and Wind Stress Curl Over the California Current. NOAA Tech. Rep. NMFS-SSRF-714, 1977.

10. Howe, J. T.: Analysis of Coastal Upwelling and the Production of a Biomass. NASA TM 78614, 1979.

11. Howe, J. T.; and McCulley, L. D.: Volume Reflecting Heatshields for Entry in the Giant Planet Atmospheres. Progress in Astronautics and Aeronautics, vol. 39, 1975, pp. 349-371.

12. Howe, J. T.; Green, M. J.; and Weston, K. C.: Thermal Shielding by Subliming Volume Reflectors in Convective and Intense Radiative Environments. AIAA Journal, vol. 11, no. 7, 1973, pp. 989-994.

13. Schuster, A.: Radiation Through a Foggy Atmosphere. The Astrophysical Journal, vol. 21, no. 1, Jan. 1905, pp. 1-22.

14. Kubelka, P.; and Munk, R.: Zeitschrift für Technische Physik, Vol. 12, 1983, p. 593.

15. Streeter, V. L.: Fluid Dynamics. McGraw-Hill, New York, 1948.

16. Ekman, V. W.: On the Influence of the Earth's Rotation on Ocean Currents. Ark. f. Mat. Astr. och Fysik. K. Sv. Vet. Ak., Stockholm 1905-1906, vol. 2, no. 11, 1905.

17. McEwen, G. F.: The Distribution of Ocean Temperatures Along the West Coast of North America Deduced from Ekman's Theory of the Upwelling of Cold Water from the Adjacent Ocean Depths. Intern. Revue ges Hydrobiol. u Hydrogr., Bd. 5, 1912, pp. 243-286.

18. Sverdrup, H. U.: Oceanography for Meteorologists. Prentice-Hall, New York, 1942.

19. Pedlosky, J.: On Coastal Jets and Upwelling in Bounded Basins. Journal of Physical Oceanography, vol. 4, no. 1, 1974, pp. 3-18.

20. Hsueh, Y.; and Kenney, R. N. III: Steady Coastal Upwelling in a Continuously Stratefied Ocean. J. Phys. Oceanogr., vol. 2, no. 1, 1972, pp. 27-33.

21. Smith, R. L.: Upwelling, Oceanography, Marine Biology. Ann. Rev., vol. 6, 1968, pp. 11-46.

22. Samuels, W. B.; and Huang, N. E.: An Oilspill Trajectory Analysis Model with a Variable Wind Deflection Angle. Ocean Engineering, vol. 9, no. 4, 1982, pp. 347-360.

23. Jerlov, N. G.: Optical Oceanography. Elsevier Publishing Co., Amsterdam, 1968.

24. McLellan, H. J.: Elements of Physical Oceanography, Pergamon Press, New York, 1965.

25. Codispotti, L. A.: Nitrogen in Upwelling Systems, Nitrogen in the Marine Environment. Carpenter, E. J. and Capone, D. G., eds., Academic Press, New York, 1983, p. 540.

26. Sverdrup, H. U.; Johnson, M. W.; and Fleming, R. H.: The Oceans. Prentice-Hall, Inc., Englewood Cliffs, New Jersey, 1942.

27. List, R. J.: American Institute of Physics Handbook, Second Ed., McGraw-Hill, New York, 1963, pp. 2-142.

28. Nitrogen in the Marine Environment. Academic Press, Inc., New York, 1983.

29. Nolton, J. W.: In Situ Optical Methods for Chlorophyll Estimation in the Sea. Thesis, Moss Landing Marine Laboratories and Department of Biology, San Jose State University, 1980.

30. Stuart, D. W.; and Linn, M. A.: Meteorological and Aircraft Data for OPUS 1981. National Science Foundation ref. FSU-MET-OPUS-83-1, 1983.

31. Starkey, R. J., Jr.: Antisubmarine Warfare Oceanography, Part II. Military Electronics/Countermeasures, p. 65, June 1981.

32. Denman, K. L.; and Platt, T.: Biological Prediction in the Sea. Contribution to NATO Advanced Study Institute on Modeling and Prediction of the Upper Layers of the Ocean, Urbino, Italy, 1975.

1. Report No.	2. Government Accession No.	3. Recipient's Catalog No.
NASA TM-88230		

4. Title and Subtitle	5. Report Date
BIOGEOCHEMICAL CYCLING IN THE OCEAN PART 1: INTRODUCTION TO THE EFFECTS OF UPWELLING ALONG THE WEST COAST OF NORTH AMERICA	May 1986
	6. Performing Organization Code
7. Author(s) John T. Howe	8. Performing Organization Report No. A-86181
	10. Work Unit No.
9. Performing Organization Name and Address Ames Research Center Moffett Field, CA 94035	11. Contract or Grant No.
	13. Type of Report and Period Covered Technical Memorandum
12. Sponsoring Agency Name and Address National Aeronautics and Space Administration Washington, DC 20546	14. Sponsoring Agency Code 506-40-11

15. Supplementary Notes

Point of contact: John Howe, Ames Research Center, MS 229-4, Moffett Field, CA 94035 (415)694-6113 or FTS 464-6113

16. Abstract Coastal upwelling is examined as it relates to the cycling of chemical species in coastal waters along the west coast of the North American continent. The temporal and spatial features of upwelling phenomena in the Eastern boundary regions of the North Pacific Ocean are presented and discussed in terms of upwelling episodes. Climate conditions that affect upwelling include: thermal effects, wind-induced shear stress which moves surface layers of water, and the curl of the wind stress vector which is thought to affect the extent and nature of upwelling and the formation of offshore convergent downwelling fronts. These effects and the interaction of sunlight and upwelled nutrients which result in a biological bloom in surface waters is modeled analytically. The roles of biological and chemical species, including the effects of predation, are discussed in that context, and relevant remote sensing and in situ observations are presented. Climatological, oceanographic, biological, physical, chemical events, and processes that pertain to biogeochemical cycling are presented and described by a set of partial differential equations. Simple preliminary results are obtained and are compared with data. Thus a fairly general framework has been laid where the many facets of biogeochemical cycling in coastal upwelled waters can be examined in their relationship to one another, and to the whole, to whatever level of detail or approximation is warranted or desired.

17. Key Words (Suggested by Author(s))	18. Distribution Statement
Biogeochemical cycling Coastal upwelling	Unlimited Subject category - 48

19. Security Classif. (of this report)	20. Security Classif. (of this page)	21. No. of Pages	22. Price*
Unclassified	Unclassified	39	

*For sale by the National Technical Information Service, Springfield, Virginia 22161